ICCES, vol.24, no.1

Tech Science Press

DOI: 10.32604/icces.2022.08695

PROCEEDINGS

Dynamic Behaviors after Droplet Impact onto Liquid Surface

Kazuhiko Kakuda[1,*] and Asuka Iizumi[1]

[1]Department of Mathematical Information Engineering, College of Industrial Technology, Nihon University, Narashino, Chiba 275-8575, Japan

[*]Corresponding Author: Kazuhiko Kakuda. Email: kakuda.kazuhiko@nihon-u.ac.jp

ABSTRACT

In this paper, we present the dynamic behaviors of crown formation, central jet, and secondary droplets generated with droplet impact onto a liquid surface by using experimental and computational approaches. In our experiment, the dynamic behaviors after a droplet impact are recorded using a high-speed camera with appropriate resolution and exposure time. On the other hand, we simulate numerically the similar behaviors using the VOF (volume of fluid) solver in the OpenFOAM. As a fluid field, we consider the multiphase flows with free surfaces based on incompressible Navier-Stokes equations in the software codes. Some qualitative comparisons between the experimental and the computational results demonstrate the workability and validity of the present approaches.

KEYWORDS

Droplet impact; liquid surface; experimental; OpenFOAM; crown formation; Worthington jet; secondary droplets

1 Introduction

The phenomena of droplet impact onto a liquid surface have some interesting behaviors such as crown formation, the cavity growth, Worthington jet (or central jet) [1], and droplet re-generation so-called secondary droplet. From a practical point of view, the clarifying the phenomena of droplet-falling impact is also important in the wide fields of science and engineering, such as inkjet printing [2], microfabrication of 3D structures [3], droplet impingement erosion in nuclear power plants [4], bloodstain pattern properties [5], and so forth. There have been many experimental and computational studies on the dynamic behaviors after a droplet impinging [6–10].

The purpose of this paper is to present experimentally and computationally the dynamic behaviors after a droplet impact onto a liquid surface, such as crown formation, central jet, and secondary droplets. After the description of the experimental setup equipping a high-speed camera, the qualitative behaviors from crown formation up to secondary droplets splashing are presented for target liquid depth with high Weber number. In the computational approach, we utilize the well-known OpenFOAM [11] as the open-source CFD software, and also adopt the multiphase-flow solver with free surfaces by using VOF method [12] in the OpenFOAM®v7. The applicability and validity of the present approaches are qualitatively demonstrated on through comparison between the experimental and the computational results.

2 Experimental Approach

2.1 Experimental Setup and Its Configuration

The configuration of the experimental setup is schematically shown in Fig.1. The studio box for photography equipped with 1,600lm LED is utilized in our experiments. The size of the box with an opening at the top is about W445mm×D580mm×H435mm. As the container to receive a droplet, a circular transparent petri dish with a diameter of 152mm and thickness of 28mm is used herein. A droplet is manually generated using the dropper. The high-speed camera (As One, 9501; Sensor Type: Python1300) employed herein has a maximum framing rate of 2,420 frames/s with a resolution of 256 × 256 pixels and a minimum exposure time of 100μs. The experiments are actually recorded at 346 frames/s with a resolution of 1024 × 768 pixels and 1ms exposure time. All the experiments are carried out at room temperature of 28.0 ℃ $\pm$ 0.5℃ and humidity of about 45%. The liquids used in this study are milk, and the specification of experimental parameters is also summarized in Tab.1.

Especially, Weber number and Ohnesorge number are well-known as parameters that characterize the dynamics of droplet impact. The Weber number, $We = \rho_l v_0^2 d_0/\sigma$, is a dimensionless number related to the inertia to the surface tension, and the Ohnesorge number, $Oh = \mu_l/\sqrt{\sigma \rho_l d_0} = \sqrt{We}/Re$, is a dimensionless number with respect to the ration of the viscosity to the surface tension, where $\rho_l, \mu_l,$ and σ are the density, the viscosity, and the surface tension of the liquids, respectively, and also d_0, v_0 and Re are the droplet diameter, the impact velocity, and the Reynolds number, respectively.

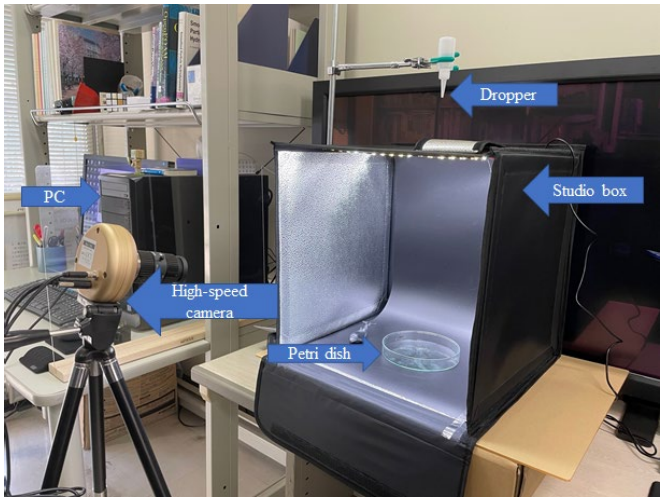

Figure 1: Configuration of experimental setup

Table 1: Summary of experimental parameters

Density, $\rho_l (kg/m^3)$	1030
Dynamic viscosity, v_l $(Pa \cdot s)$	1.70×10^{-6}
Surface tension, σ (N/m)	0.054
Impact velocity, v_0 (m/s)	3.13
Droplet diameter, d_0 (mm)	3.5
Liquid depth, h (mm)	6.0
Weber number, *We*	654.03
Ohnesorge number, *Oh*	0.0039686
Reynolds number, *Re*	6444.1

3 Computational Approach

3.1 Statement of Problem

Let Ω be a bounded domain in Euclidean space R with a piecewise smooth boundary Γ. The unit outward normal vector to Γ is denoted by n. Also, $\Im$ denotes a closed time interval. The motion of a viscous fluid flow is governed by the following incompressible Navier-Stokes equations for Eulerian form:

$$\frac{\partial \boldsymbol{u}}{\partial t} + \boldsymbol{u} \cdot \nabla \boldsymbol{u} = -\frac{1}{\rho}\nabla p + \nu \nabla^2 \boldsymbol{u} + \boldsymbol{g} + \boldsymbol{f}^{surf} \qquad in\ \Im \times \Omega \tag{1}$$

$$\nabla \cdot \boldsymbol{u} = 0 \qquad in\ \Im \times \Omega \tag{2}$$

where $\boldsymbol{u}$ is the velocity vector, p is the pressure, ρ is the density, $\nu = \mu/\rho$ is the kinematic viscosity coefficient, μ is the viscosity coefficient, $\boldsymbol{g}$ is the external force vector, e.g., gravity, and $\boldsymbol{f}^{surf}$ is the surface tension vector. In addition to Eqs. (1) and (2), we prescribe the Dirichlet and Neumann boundary conditions, and the initial condition, $\boldsymbol{u}(x, 0) = \boldsymbol{u}^0$, where $\boldsymbol{u}^0$ denotes the given initial velocity vector.

3.2 Numerical Simulation Using OpenFOAM

We utilize the well-known OpenFOAM [9] as the open-source CFD software to generate fluid flow datasets. There are various fields of topics in OpenFOAM software, such as incompressible, compressible, turbulent and multiphase flows, and so on. This software has also the grid-based and particle-based methods. Because of its suitability for grid-based discretization approach with respect to the droplet impact, we adopt the multiphase flows with free surfaces by VOF method [11] in the OpenFOAM®v7. In addition to Eqs. (1) and (2) as the VOF approach, we consider the following transport equation for multi-phase systems

$$\frac{\partial \alpha}{\partial t} + \nabla \cdot (\alpha \boldsymbol{u}) + \nabla \cdot [(1-\alpha)\alpha \boldsymbol{u}_r] = 0 \qquad in\ \Im \times \Omega \tag{3}$$

where α is the phase fraction, and $\boldsymbol{u}_r$ is the relative velocity vector for the multi-phase fluid flows. The CSF (Continuous Surface Force) model involving the curvature calculation is used for the surface tension, $\boldsymbol{f}^{surf} = \sigma\kappa\nabla\alpha$, in which σ is the surface tension coefficient, and κ denotes the curvature of the interface.

The computational domain constrained by the boundary conditions is 30mm×30mm×60mm with 6,750,000 grid-cells as shown in Fig. 2. In the numerical simulation, the droplet and the target liquid surrounding by air are configured by means of the same liquid (milk) as the experimental study (see Tables 1 and 2).

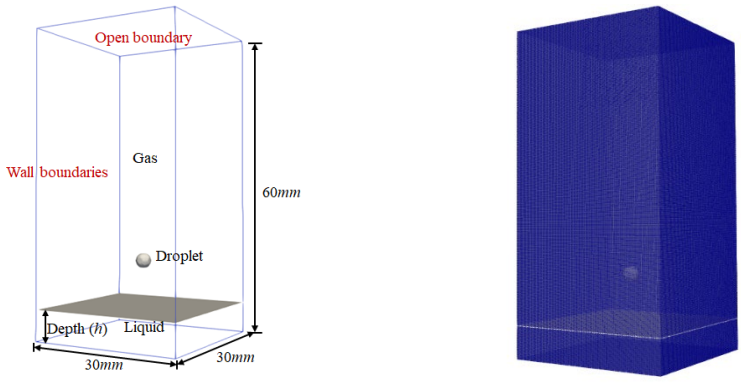

(a) Computational domain and boundary conditions (b) Grid-cells representation

Figure 2: Configuration of computational approach

Table 2: Summary of gas(air)-phase parameters

Density, $\rho_g(kg/m^3)$	1.0
Dynamic viscosity, $\nu_g\ (Pa \cdot s)$	1.51×10^{-5}

3.3 Computational Results and Comparisons with Experimental data

Fig.3 shows the qualitative comparison of the computational and experimental images of time sequences after a droplet impinging onto a liquid surface. As you can see from these images, the dynamic behaviors such as crown-like formation, central jet, so-called Worthington jet, and multiple (i.e., four) secondary droplets are obtained experimentally and also computationally for high Weber number. The qualitative consistency of both approaches appears satisfactorily.

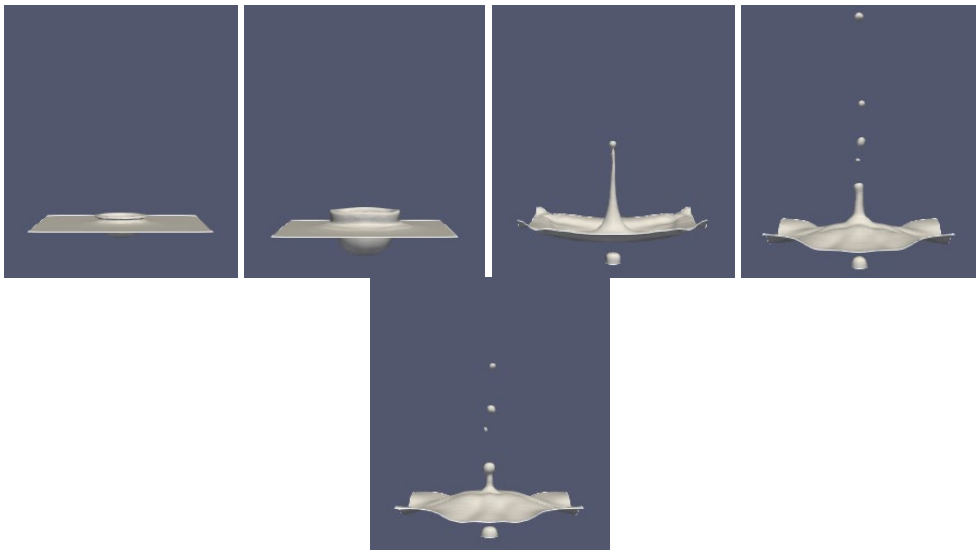

(a) Computational results

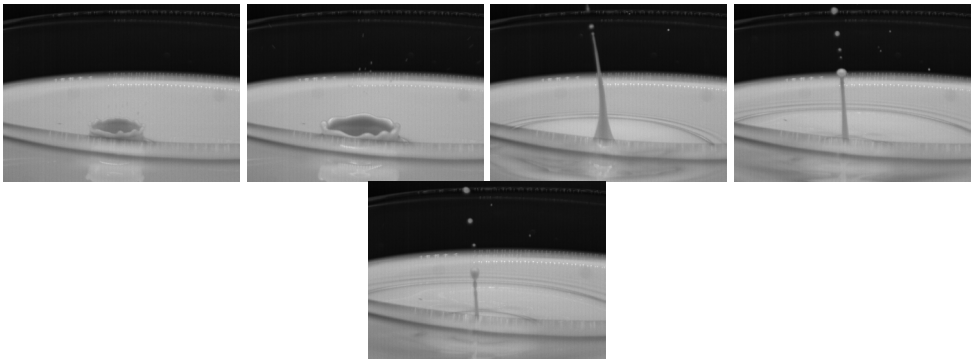

(b) Experimental results

Figure 3: Qualitative comparison of the computational and experimental images of time sequences after a droplet impact ($We = 654.03, v_0 = 3.13\,m/s\,, h = 6.0mm$)

4 Conclusions

We have presented experimentally and computationally the dynamic behaviors after a droplet impact onto a liquid surface. The dynamic behaviors after a droplet impact were experimentally recorded using a high-speed camera with appropriate resolution and exposure time. As the computational approach, we have adopted the VOF solver in the OpenFOAM of the open-source CFD software. The agreement between the computational and the experimental approaches appears

qualitatively satisfactory.

References

1. Worthington, A. M. (1908). *A study of splashes*. Longmans, Green and Co, Forgotten Books.
2. van der Bos, A., van der Meulen, M.-J., Driessen, T., van den Berg, M., Reinten, H., Wijshoff, H., Versluis, M., Lohse, D. (2014). Velocity profile inside piezoacoustic inkjet droplets in flight: comparison between experiment and numerical simulation. *Physical Review Applied, 1*, 014004.
3. Antkowiak, A., Audoly, B., Josserand, C., Neukirch, S., Rivetti, M. (2011). Instant fabrication and selection of folded structures using drop impact. *Proceedings of the National Academy of Sciences, 108(26)*, 10400–10404.
4. Fujisawa, N., Yamagata, T., Hayashi, K., Takano, T. (2012). Experiments on liquid droplet impingement erosion by high-speed spray. *Nuclear Engineering and Design, 250*, 101–107.
5. Laan, N., de Bruin, K.G., Bartolo, D., Josserand, C., Bonn, D. (2014). Maximum diameter of impacting liquid droplets. *Physical Review Applied, 2*, 044018.
6. Castillo-Orozco, E., Davanlou, A., Choudhury, P.K., Kumar, R. (2015). Droplet impact on deep liquid pools: Rayleigh jet to formation of secondary droplets. *Physical Review E, 92*, 053022.
7. Engel, O. G. (1967). Initial pressure, initial flow velocity, and the time dependence of crater depth in fluid impacts. *Journal of Applied Physics, 38(10)*, 3935–3940.
8. Liow, J. L. (2001). Splash formation by spherical drops. *Journal of Fluid Mechanics, 427*, 73–105.
9. Harlow, F. H., Shannon, J. P. (1967). The splash of a liquid drop. *Journal of Applied Physics, 38*, 3855–3866.
10. Ma, H., Liu, C., Li, X., Huang, H., Dong, J. (2019). Deformation characteristics and energy conversion during droplet impact on a water surface. *Physics of Fluids, 31*, 062108.
11. OpenFOAM®-The open source computational fluid dynamics (CFD) toolbox, http://www.openfoam.com.
12. Weller, H. G. (2008). A new approach to VOF-based interface capturing methods for incompressible and compressible flow. *Technical Report TR/HGW/04*.